BER Upper Bound Expressions in Coded Two-Transmission Schemes With Arbitrarily Spaced Signal Constellations

Mehmet Cagri Ilter, Halim Yanikomeroglu, and Pawel A. Dmochowski

***Abstract*—The main contribution of this letter is the derivation of an upper bound BER expression, as a function of distances between signal points, for arbitrary constellations, in a generic, two-transmission scheme such as relaying, HARQ, or CoMP. The approach utilizes the product-state matrix, and thus the arbitrarily chosen constellations together with the encoders do not need to satisfy the quasi-regularity property that includes geometrical uniformity and symmetry. The channel fading is modeled using a Nakagami-*m* distribution, both with and without correlation between the two transmissions. We also allow for different path loss at each transmission. The results are valid for general coded schemes as long as a transfer function expression can be derived (convolutional codes and trellis coded modulation). The upper bounds are very accurate for BER values lower than 10^{-2} for any chosen constellation.**

***Index Terms*—Channel coding, constellation diagram, convolutional codes.**

I. Introduction

DUE to the ability to mitigate the adverse effects of radio-wave propagation, such as fading and shadowing, convolutional encoding has been extensively studied and utilized in a wide range of wireless systems. While early research on their performance analysis naturally focused on point-to-point communications [1], present day applications call for more advanced architectures such as point-to-multipoint and multipoint-to-multipoint. To model scenarios such as CoMP (coordinated multipoint transmission), HARQ, and relaying, a generic of multi transmission has recently been proposed [2]–[4].

Most studies of coded scenarios are restricted to systems satisfying the uniform error property, [2], [4], [5], i.e., they assume equal weight distance spectrum for every codeword regardless of the sequences transmitted. Consequently, they assume a quasi-regular (QR) encoder-constellation pair, such as geometrically uniform codes [6]. With this restriction, the performance analysis of systems with coding schemes (e.g., convolutional codes and trellis coded modulation (TCM)) utilizes the transfer function calculation method described in digital communication textbooks, such as similar to that in classical systems [1]. In [2], a Euclidean distance-based BER upper bound was derived for coded maximal ratio combining (MRC) systems in Nakagami-*m* channel. In [4] a similar technique is used for the studied generic multi-transmission scheme under the assumption that no inter-transmission correlation exists.

Recent increase in the availability of advanced optimization techniques to physical layer researchers has resulted in renewed interest in a number of classic digital communications problems, including constellation optimization [7]–[9]. Unfortunately, the above conventional BER analysis is valid only when the combination of the encoder and the constellation is quasi-regular [6].[1]

In this letter we addresses this very problem. Rather than adopting the conventional transfer function calculation technique previously used in the literature (such as [2], [4], [5]), we utilize the product-state matrix technique adapted from [11] to calculate the transfer function expression. The product-state matrix technique allows us to develop very tight error bounds for coded systems with completely arbitrary signal constellations, making them suitable for far-reaching constellation optimization applications.[2]

Specifically, the contribution of this letter is the derivation of a very tight BER upper bound for a coded, two-transmission system (modelling CoMP, HARQ or relaying) operating in a Nakagami-*m* fading environment for any encoder-constellation pair as long as a transfer function can be written. Unlike previous approaches, the proposed method calculates the transfer function based on the product-state matrix technique which does not require the constellation and encoder to satisfy the quasi-regularity. We derive the expressions for the branch label of the product-state matrix, in the presence of correlated fading between the two transmission phases.

II. System Architecture

We consilder a system architecture consisting of two orthogonal transmission phases as shown in Fig. 1 where each transmitter employs the same convolutional encoder, but not necessarily the same constellation. During each transmission phase, the same information bit sequence is first coded by a rate R convolutional encoder, and the resulting bits are assigned a signal point from an arbitrary M-ary constellation based on a bit-to-symbol mapping rule. Note that throughout this letter, the natural mapping is employed[3].

The mapper output symbols $\{s^{(i)}\}$, $i = 1, 2$, where i refers to the transmission phase, are transmitted. The corresponding received signals are given by $r_i = h_i s^{(i)} + n_i$, where h_i, $i \in \{1, 2\}$, denotes frequency non-selective Nakagami-*m* fading coefficient with shaping parameter m_i and average fading power Ω_i; n_i is the additive white Gaussian noise (AWGN) sample with zero-mean and $N_0/2$ variance per dimension. Note that we allow the channel parameters to

Manuscript received July 21, 2015; accepted December 22, 2015. Date of publication December 31, 2015; date of current version February 12, 2016. This work is supported in part by Huawei Canada Co., Ltd., and in part by the Ontario Ministry of Economic Development and Innovation's ORF-RE (Ontario Research Fund-Research Excellence) Program. The associate editor coordinating the review of this paper and approving it for publication was A. Ikhlef.

M. C. Ilter and H. Yanikomeroglu are with the Department of Systems and Computer Engineering, Carleton University, Ottawa, ON K1S5B6, Canada (e-mail: ilterm@sce.carleton.ca).

P. A. Dmochowski is with the School of Engineering and Computer Science, Victoria University of Wellington, Wellington 6140, New Zealand.

Digital Object Identifier 10.1109/LCOMM.2015.2513775

[1] It was noted in [10] that the quasi-regularity does not necessarily result in better performance.

[2] Constellation optimization is beyond the scope of this letter.

[3] For instance, in a 64-ary signalling scheme, s_{60} corresponds to the following 6 bits: 111100.

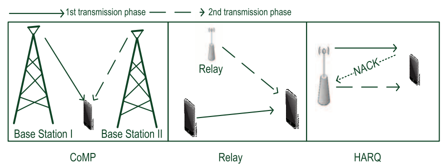

Fig. 1. Possible system realizations for the two orthogonal transmission scheme.

vary between the transmission phases and that each symbol is exposed to a different fading coefficient. Independent fading between the phases is considered first followed by the analysis for the correlated case, where the correlation coefficient between h_1 and h_2, is defined as $\rho = \text{cov}\left(|h_1|^2, |h_2|^2\right)/\sqrt{\text{var}\left(|h_1|^2\right)\text{var}\left(|h_2|^2\right)}$, $\rho \in [0, 1]$.

III. Calculation of Product-State Matrix and Upper Bound BER Expression

We now derive the upper bound BER for the coded two-orthogonal transmission model described in Section II. In doing so, we begin with the commonly known BER upper bound for an encoder with a transfer function $T(D, I)$ [12, (9)]

$$P_b \leq \frac{1}{k}\frac{\partial}{\partial I} T(D, I)\bigg|_{I=1}. \tag{1}$$

The calculation of $T(D, I)$ can differ based on the encoder and constellation used. The popular transfer function calculation method which appears in many digital communications textbooks (such as [1]) is only valid under the assumption of quasi-regularity. In 1984, Biglieri proposed a general method which can be readily used for both quasi-regular (QR) and non-QR cases [11] (for details of quasi-regularity please refer to [6]).

A. Calculation of Product-State Matrix and Transfer Function

For an N-state convolutional encoder, N^2 ordered pairs of product-states (u, v), can be defined where u is the encoder state and v is the decoder state selected by the Viterbi decoder ($u, v \in \{1, \ldots, N\}$). Consider a $N^2 \times N^2$ product-state matrix $\mathbf{S}(D, I)$ with entries based on transitions from (u, v) to $(\bar{u}, \bar{v})$. Using the notation in [11], the product-states can be divided into two categories: 'good states' $\mathcal{G}$ where $u = v$ (the encoder and the decoder states are the same), and 'bad states' $\mathcal{B}$ where $u \neq v$. Using this classification and suitably ordering the product-states, $\mathbf{S}(D, I)$ can be written as [11]

$$\mathbf{S}(D, I) = \begin{bmatrix} \mathbf{S}_{\mathcal{G}\mathcal{G}}(D, I) & \mathbf{S}_{\mathcal{G}\mathcal{B}}(D, I) \\ \mathbf{S}_{\mathcal{B}\mathcal{G}}(D, I) & \mathbf{S}_{\mathcal{B}\mathcal{B}}(D, I) \end{bmatrix}. \tag{2}$$

Here, $\mathbf{S}_{\mathcal{G}\mathcal{G}}(D, I)$ and $\mathbf{S}_{\mathcal{B}\mathcal{B}}(D, I)$ include the transitions for $\mathcal{G} \to \mathcal{G}$ and $\mathcal{B} \to \mathcal{B}$, respectively. Likewise, $\mathbf{S}_{\mathcal{B}\mathcal{G}}(D, I)$ represents the transition for $\mathcal{B} \to \mathcal{G}$ and so forth. Let $D_{(u,v),(\bar{u},\bar{v})}$ denote the branch label for transition $(u \to \bar{u})$ and $(v \to \bar{v})$. It was shown in [13] that each entry of $\mathbf{S}(D, I)$ can be written as

$$[\mathbf{S}(D, I)]_{(u,v),(\bar{u},\bar{v})} = p(u \to \bar{u}|u) \times \sum_n p_n I^{a(u\to\bar{u})\oplus a(v\to\bar{v})} D_{(u,v),(\bar{u},\bar{v})}, \tag{3}$$

assuming both transitions $(u \to \bar{u})$ and $(v \to \bar{v})$ exist, otherwise $[\mathbf{S}(D, I)]_{(u,v),(\bar{u},\bar{v})} = 0$. The summation in (3) is over possible n parallel transitions depending on a given encoder, where p_n denotes the probability of nth parallel transition between $(u \to \bar{u})$ if it exists, otherwise $p_n = 1$. In (3), $p(u \to \bar{u}|u)$ is the conditional probability of transition from state u to state $\bar{u}$ given state u, $a(u \to \bar{u})$ denotes the Hamming weight of the information sequence for the transition from u to $\bar{u}$ [13]. Using the partitioning in (2), the transfer function can be calculated as [11]

$$T(D, I) = \mathbf{a} + \mathbf{b}^T\left[\mathbf{I} - S_{\mathcal{B}\mathcal{B}}(D, I)\right]^{-1}\mathbf{c}, \tag{4}$$

where $\mathbf{a} = \mathbf{1}^T\mathbf{S}_{\mathcal{G}\mathcal{G}}(D, I)\,\mathbf{1}$, $\mathbf{b} = \mathbf{1}^T\mathbf{S}_{\mathcal{G}\mathcal{B}}(D, I)$, and $\mathbf{c} = \mathbf{S}_{\mathcal{B}\mathcal{G}}(D, I)\,\mathbf{1}$. Here, $\mathbf{1}$ and $\mathbf{I}$ denote a unity matrix and identity matrix, respectively. Then, $\partial T(D, I)/\partial I$ in (1) can be expressed as

$$\begin{aligned}\frac{\partial T(D, I)}{\partial I} = \frac{1}{2N}\Big(&\mathbf{a}' + \mathbf{b}'^T\left[\mathbf{I} - \mathbf{S}_{\mathcal{B}\mathcal{B}}(D, I)\right]^{-1}\mathbf{c} \\ &+ \mathbf{b}^T\left[\mathbf{I} - \mathbf{S}_{\mathcal{B}\mathcal{B}}(D, I)\right]^{-1}\mathbf{c}' + \mathbf{b}^T\left[\mathbf{I} - \mathbf{S}_{\mathcal{B}\mathcal{B}}(D, I)\right]^{-1} \\ &\mathbf{S}_{\mathcal{B}\mathcal{B}}(D, I)'\left[\mathbf{I} - \mathbf{S}_{\mathcal{B}\mathcal{B}}(D, I)\right]^{-1}\mathbf{c}\Big),\end{aligned} \tag{5}$$

where $(\cdot)'$ denotes element-wise derivative with respect to I.

B. Calculation of $D_{(u,v),(\bar{u},\bar{v})}$

Note that $D_{(u,v),(\bar{u},\bar{v})}$ in (3) can be interpreted as the Bhattacharyya parameter representing possibility of decoding the erroneous transition $(v \to \bar{v})$ rather than the correct one $(u \to \bar{u})$ under ML (maximum likelihood) decoding [11]. For a given bit-to-symbol mapper $g(\cdot)$ and corresponding binary label of a specified transition $b(\cdot)$, $D_{(u,v),(\bar{u},\bar{v})}$ is a function of the distances between the output symbols $s^{(i)} = g(b(u \to \bar{u}))$ and the erroneously decoded symbols $\hat{s}^{(i)} = g(b(v \to \bar{v}))$ for each transmission phase $i \in \{1, 2\}$. For a given channel coefficient set, $\{h_1, h_2\}$, $D_{(u,v),(\bar{u},\bar{v})}$ can be explicitly written as[4]

$$D_{(u,v),(\bar{u},\bar{v})|\{\gamma_1,\gamma_2\}} = \exp\{-d_1\gamma_1 - d_2\gamma_2\}, \tag{6}$$

where $d_i = \left|s^{(i)} - \hat{s}^{(i)}\right|^2/4N_0$ and $\gamma_i = |h_i|^2$. Averaging (6) over the channel statistics yields $D_{(u,v),(\bar{u},\bar{v})}$ which we use to obtain each entry of (2) which in turn will be used to compute the upper bound BER using (5) and (1).

We now derive $D_{(u,v),(\bar{u},\bar{v})}$ expression for Nakagami-m fading scenarios with and without correlation between transmission phases. From (6), the unconditional Bhattacharyya parameter for the case of uncorrelated transmission phases can be written as

$$D_{(u,v),(\bar{u},\bar{v})} = \int_0^\infty\int_0^\infty d\gamma_1 d\gamma_2 \exp\{-(d_1\gamma_1 + d_2\gamma_2)\} f_{\gamma_1,\gamma_2}(\gamma_1, \gamma_2), \tag{7}$$

where $f_\gamma(\gamma_1, \gamma_2)$ denotes the joint PDF of γ_1 and γ_2.

1) Uncorrelated Case $(\rho = 0)$*:* Here, the joint pdf is simply $f_\gamma(\gamma_1, \gamma_2) = f_\gamma(\gamma_1)\,f_\gamma(\gamma_2)$, where $f_\gamma(\gamma_i)$ denotes the probability density function of the squared envelope of Nakagami-faded channel coefficient, known to follow the Gamma distribution [14]

$$f_{\gamma_i}(\gamma) = \frac{\gamma^{m_i-1}e^{-\gamma\frac{m_i}{\Omega_i}}}{\Omega_i{}^{m_i}m_i{}^{-m_i}\Gamma(m_i)}, \tag{8}$$

[4]The derivation of (6) is rather straightforward, and thus omitted here.

where Ω_i is the average fading power, $m_i \geq 0.5$, and $\Gamma(\cdot)$ is the Gamma function [15]. Combining (7)–(8) and using [15, eq. 3.35.2] one can, after some manipulation, obtain

$$D_{(u,v),(\bar{u},\bar{v})} = \left(\frac{\Omega_1 d_1}{m_1} + \Omega_1\right)^{-m_1} \left(\frac{\Omega_2 d_2}{m_2} + \Omega_2\right)^{-m_2}. \quad (9)$$

2) Correlated Case ($0 < \rho \leq 1$): Fading correlation in the two transmission phases is an important consideration, as it can arise, for example, in an HARQ retransmission within the coherence time of the channel [16]. We start by considering a special case, followed by a more general result. For $m_1 = m_2 = m$, $f_\gamma(\gamma_1, \gamma_2)$ is given by [17]

$$f_\gamma(\gamma_1, \gamma_2) = \frac{(\gamma_1\gamma_2)^{0.5m-0.5} m^{m+1} \mathrm{e}^{-\frac{m}{1-\rho}\left(\frac{\gamma_1}{\Omega_1}+\frac{\gamma_2}{\Omega_2}\right)}}{\Gamma(m)\,\Omega_1\Omega_2(1-\rho)\left(\sqrt{\rho\Omega_1\Omega_2}\right)^{m-1}} \times \mathcal{I}_{m-1}\left(\frac{2m\sqrt{\gamma_1\gamma_2\rho}}{(1-\rho)\sqrt{\Omega_1\Omega_2}}\right), \quad (10)$$

where $\mathcal{I}_{m-1}(\cdot)$ denotes the modified Bessel function of order $m-1$ [15]. For $\Omega_1 = \Omega_2 = 1$, substituting (10) into (7) and using [15, (6.643.2), (7.621.2)] lead to

$$D_{(u,v),(\bar{u},\bar{v})} = \frac{m^{2m}\left(\left(d_1+\frac{m}{1-\rho}\right)\left(d_2+\frac{m}{1-\rho}\right)-\frac{m^2\rho}{(1-\rho)^2}\right)^{-m}}{(1-\rho)^m}. \quad (11)$$

For the more general case of $m_1 \neq m_2$, $\Omega_1 \neq \Omega_2$, the joint PDF $f_\gamma(\gamma_1, \gamma_2)$ is given by [17] as

$$f_\gamma(\gamma_1, \gamma_2) = (1-\rho)^{m_2} \sum_{k=0}^{\infty} \Bigg\{ \frac{(m_1)_k \rho^k}{k!} \left(\frac{m_1}{\Omega_1(1-\rho)}\right)^{m_1+k} \times \left(\frac{m_2}{\Omega_2(1-\rho)}\right)^{m_2+k} \frac{\gamma_1^{m_1+k-1}}{\Gamma(m_1+k)} \frac{\gamma_2^{m_2+k-1}}{\Gamma(m_2+k)} \mathrm{e}^{\frac{-1}{(1-\rho)}\left(\frac{m_1\gamma_1}{\Omega_1}+\frac{m_2\gamma_2}{\Omega_2}\right)} \times {}_1F_1\left(m_2-m_1, m_2+k; \frac{\rho m_2\gamma_2}{\Omega_2(1-\rho)}\right)\Bigg\}, \quad (12)$$

where ${}_1F_1(\cdot, \cdot; \cdot)$ is the Kummer confluent hypergeometric function [15], and $(m_1)_k$ denotes the Pochhammer symbol. Substituting (12) into (7) and using [15, (3.351.2)] to integrate over γ_1, result in

$$D_{(u,v),(\bar{u},\bar{v})} = \sum_{k=0}^{\infty} C \Bigg\{ \int_0^\infty d\gamma_2 e^{-\left(\frac{m_2}{\Omega_2(1-\rho)}+\frac{d_2}{\sin^2\Phi}\right)\gamma_2} \gamma_2^{m_2+k-1} \times {}_1F_1\left(m_2-m_1, m_2+k; \frac{\rho m_2\gamma_2}{\Omega_2(1-\rho)}\right) \times \left(\frac{m_1}{\Omega_1(1-\rho)} + \frac{d_1}{\sin^2\Phi}\right)^{-m_1-k} \Gamma(m_1+k) \Bigg\}, \quad (13)$$

where C is a constant. After some rearrangement and the utilization of [15, (7.522.9)], (13) can be rewritten as

$$D_{(u,v),(\bar{u},\bar{v})} = \sum_{k=0}^{\infty} C \Bigg\{ \left(\frac{m_2}{\Omega_2(1-\rho)} + \frac{d_2}{\sin^2\Phi}\right)^{-m_2-k} \times \Gamma(m_2+k)\, {}_2F_1(m_2-m_1, m_2+k; m_2+k; M) \times \left(\frac{m_1}{\Omega_1(1-\rho)} + \frac{d_1}{\sin^2\Phi}\right)^{-m_1-k} \Gamma(m_1+k) \Bigg\}. \quad (14)$$

TABLE I

MONTE CARLO SIMULATION PARAMETERS

	Scenario	Ω_1	Ω_2	m_1	m_2	ρ
4-ary w/ $[2, 1]_8$	I	1	1	1.5	1.5	0
	II	1	1	1.5	1	0
64-ary w/ $[133, 171, 165]_8$	III	1	0.9	1	1.5	0.7
	IV	1	1	3.5	3.5	0.5
Constellation-I	$\{-2.17 + 0.14i, 0.66 - 0.84i, -0.06 + 0.29i, -062 - 0.13i\}$					
Constellation-II	$\{1.06 + 2.64i, -1.72 - 1.03i, -0.34 - 0.59i, 1.34 + 0.72i\}$					

In (14), ${}_2F_1(\cdot, \cdot; \cdot; \cdot)$ denotes the Gauss hypergeometric function [15] and M is defined as

$$M = \frac{\rho m_2}{\Omega_2(1-\rho)\left(\frac{m_2}{\Omega_2(1-\rho)} + \frac{d_{l,2}}{\sin^2\Phi}\right)}. \quad (15)$$

Finally, utilizing the identity ${}_2F_1(a, b; b; c) = (1-c)^{-a}$ [15, (9.121.1)], we obtain $D_{(u,v),(\bar{u},\bar{v})}$ as

$$D_{(u,v),(\bar{u},\bar{v})} = \sum_{k=0}^{\infty} (m_2\rho)^{k+m_2} \left(\frac{m_1}{m_1 + \Omega_1 d_1 - \Omega_1 d_1 \rho}\right)^{m_1+k} \times (m_1)_k \frac{1}{k!} (m_2 - \Omega_2 d_2(\rho-1))^{-m_1-k} \left(\frac{1}{\rho} - 1\right)^{m_2} \times (-(m_2 + \Omega_2 d_2)(\rho-1))^{m_1-m_2}. \quad (16)$$

The $D_{(u,v),(\bar{u},\bar{v})}$ expressions in (9), (11) and (16) are first substituted into (3) and then used in (5) and (1) to obtain the BER upper bound. This is computed in the following section.

IV. NUMERICAL SCENARIOS

We now present simulation results to validate the upper bound BER expressions derived in Section III. We consider 4-ary and 64-ary signalling. The selected convolutional encoders, along with the values of other key parameters are listed in Fig. 1. The infinite sum in (16) for the case of correlated fading with $m_1 \neq m_2$ was truncated after 15 terms.

A. Arbitrary 4-Ary Signalling

We first consider Scenarios I and II with 4-ary signalling and a rate $R = 1/2$ convolutional encoder $[2, 1]_8$. The arbitrary 4-ary constellations given in Table I were obtained using a random number generator. Based on the QR criteria described in [6], Constellation-I in conjunction with the above encoder results in a non-QR system. In contrast, to enable a comparison to the previous bounds in the literature which are obtained based on the transfer function ([2], [4]), Constellation-II was chosen to satisfy QR. The constellations were fixed between transmission phases. Fig. 2 shows the BER obtained by simulation and the developed upper bound BER expression using (1) with (9) as well as the BER bound obtained by the conventional transfer function calculation [2], [4].

As it can be seen from Fig. 2, the proposed BER bound expression is very tight for both QR and non-QR scenarios. For the QR case (Scenario II), the conventional and proposed methods are almost identical, but as expected, the conventional bound fails to predict the performance of the non-QR scenario.

B. Arbitrary 64-Ary Signalling

Scenarios III and IV consider 64-ary signalling and a rate $R = 1/3$ convolutional encoder, $[133, 171, 165]_8$, deployed in

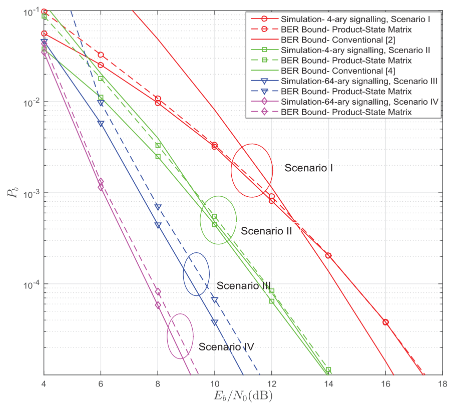

Fig. 2. Bit error probability of the two-transmission scheme for arbitrary 4-ary and 64-ary signalling.

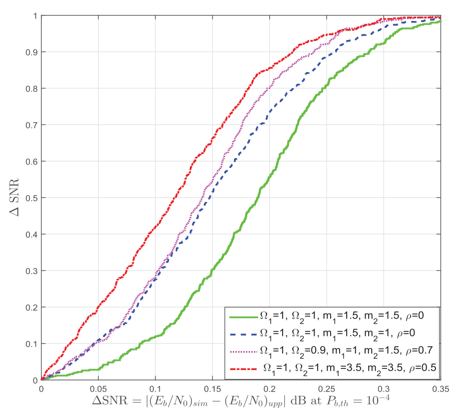

Fig. 3. CDF of ΔSNR over 500 random constellation realizations for 4-ary signalling.

downlink control information (DCI) specified in the 3GPP LTE standard [18]. To generate arbitrary 64-ary constellations, the rotation technique in [12] was used, with $\theta = 0$ and $\pi/5$, and $\theta = 0$ and $\pi/8$, for transmission phases 1 and 2, respectively. Note that we were unable to generate a 64-ary constellation which satisfies QR when paired with above coder. Scenario III features a 0.46 dB SNR difference between the received signal levels in the transmission phases. As seen in Fig. 2, the upper bounds obtained by (11) and (16) show good agreement with the simulated BER results in moderate and high SNR regions. It is seen that for the scenarios considered, the BER upper bounds are fairly tight in the high SNR regions with BER $\leq 10^{-2}$.

C. Upper Bound BER Tightness Measure

Due to the space limitations, simulation results in Section IV-A, B consider only a few specific scenarios. In this section, we evaluate the BER bound accuracy for a large number of randomly generated 4-ary constellations. Specifically, for a BER target, $P_{b,th}$, we calculate the error ΔSNR between the actual, simulated SNR required for $P_{b,th}$, and the SNR obtained using the bound derived in Section III. By plotting the CDF of ΔSNR, the characteristics of both the uncorrelated and correlated expressions can be investigated for a broad range of constellation pairs. As seen in Fig. 3, the proposed upper bound BER expressions show better agreement for uncorrelated cases with both equal and unequal Nakagami-*m* shaping parameters. The SNR discrepancy obtained is limited to around 0.3 dB. Thus, the proposed method performs well over most of the realizations.

V. Conclusions

We have presented a very tight upper bound BER expression for convolutional coded two-transmission signalling. In contrast to previous work, our method applies to generic 2D constellations and is not limited to those satisfying the quasi-regularity. We have derived the branch label expressions given in (9), (11), and (16) to generate the product-state matrix used in the transfer function calculation. Since the upper bound BER expressions presented here only require a generic transfer function for a given encoder (i.e., convolutional and trellis coded modulation codes), the results can be utilized in constellation searches over various coded two-transmission scenarios.

References

[1] A. Viterbi and J. Omura, *Principle of Digital Communication and Coding*. New York, NY, USA: McGraw-Hill, 1979.
[2] S. Zummo, "Union bounds on the bit error probability of coded MRC in Nakagami-m fading," *IEEE Commun. Lett.*, vol. 10, no. 11, pp. 769–771, Nov. 2006.
[3] H.-T. Pai, Y. S. Han, and Y.-J. Chu, "New HARQ scheme based on decoding of tail-biting convolutional codes in IEEE 802.16e," *IEEE Trans. Veh. Technol.*, vol. 60, no. 3, pp. 912–918, Mar. 2011.
[4] M. C. Ilter and H. Yanikomeroglu, "An upper bound on BER in a coded two-transmission scheme with same-size arbitrary 2D constellations," in *Proc. IEEE 25th Annu. Int. Symp. Pers. Indoor Mobile Radio Commun. (PIMRC)*, Sep. 2014, pp. 687–691.
[5] X. Zhang, Y. Zhao, and L. Zou, "Optimum asymmetric constellation design for trellis-coded modulation over Gaussian channels," *IEEE Commun. Lett.*, vol. 13, no. 7, pp. 528–530, Jul. 2009.
[6] S. Benedetto, M. Mondin, and G. Montorsi, "Performance evaluation of trellis-coded modulation schemes," *Proc. IEEE*, vol. 82, no. 6, pp. 833–855, Jun. 1994.
[7] J.-E. Porath and T. Aulin, "Design of multidimensional signal constellations," *IEE Proc. Commun.*, vol. 150, no. 5, pp. 317–323, Oct. 2003.
[8] F. Kayhan and G. Montorsi, "Joint signal-labeling optimization under peak power constraint," *Int. J. Satell. Commun. Netw.*, vol. 30, no. 6, pp. 251–263, Sep. 2012.
[9] C. Hager, A. Graell i Amat, A. Alvarado, and E. Agrell, "Design of APSK constellations for coherent optical channels with nonlinear phase noise," *IEEE Trans. Commun.*, vol. 61, no. 8, pp. 3362–3373, Aug. 2013.
[10] S. Nagaraj, "Performance analysis of coded SSK modulation on block fading channels," *IEEE Trans. Veh. Technol.*, doi: 10.1109/TVT.2015.2477295, to be published.
[11] E. Biglieri, "High-level modulation and coding for nonlinear satellite channels," *IEEE Trans. Commun.*, vol. 32, no. 5, pp. 616–626, May 1984.
[12] D. Divsalar, M. Simon, and J. Yuen, "Trellis coding with asymmetric modulations," *IEEE Trans. Commun.*, vol. 35, no. 2, pp. 130–141, Feb. 1987.
[13] J. Shi and R. D. Wesel, "Efficient computation of trellis code generating functions," *IEEE Trans. Commun.*, vol. 52, no. 2, pp. 219–227, Feb. 2004.
[14] M.-S. Alouini, A. Abdi, and M. Kaveh, "Sum of gamma variates and performance of wireless communication systems over Nakagami-fading channels," *IEEE Trans. Veh. Technol.*, vol. 50, no. 6, pp. 1471–1480, Nov. 2001.
[15] I. S. Gradshteyn and I. Ryzhik, *Table of Integrals, Series, and Products*, 7th ed. New York, NY, USA: Academic, 2007.
[16] S. M. Kim, W. Choi, T. W. Ban, and D. K. Sung, "Optimal rate adaptation for hybrid ARQ in time-correlated Rayleigh fading channels," *IEEE Trans. Wireless Commun.*, vol. 10, no. 3, pp. 968–979, Mar. 2011.
[17] T. Piboongungon, V. Aalo, C. Iskander, and G. Efthymoglou, "Bivariate generalised gamma distribution with arbitrary fading parameters," *Electron. Lett.*, vol. 41, no. 12, pp. 709–710, 2005.
[18] 3GPP, "Evolved Universal Terrestrial Radio Access (E-UTRA); Multiplexing and channel coding (3GPP TS 36.212 version 8.7. 0 Release 8)," Jun. 2009.